MOLECULAR AND CELLULAR BIOLOGY, Sept. 2007, p. 6309–6322 Vol. 27, No. 18
0270-7306/07/$08.00+0 doi:10.1128/MCB.00291-07


# Complementary Roles of Intracellular and Pericellular Collagen Degradation Pathways In Vivo▽†

Rebecca A. Wagenaar-Miller,[1] Lars H. Engelholm,[2] Julie Gavard,[1] Susan S. Yamada,[3] J. Silvio Gutkind,[1] Niels Behrendt,[2] Thomas H. Bugge,[1]* and Kenn Holmbeck[3]*

*Oral and Pharyngeal Cancer Branch[1] and Craniofacial and Skeletal Diseases Branch,[3] National Institute of Dental and Craniofacial Research, National Institutes of Health, 30 Convent Drive, Bethesda, Maryland 20892, and Finsen Laboratory, Rigshospitalet, Copenhagen Biocenter, Ole Maaløe Vej 5, DK-2200 Copenhagen N, Denmark[2]*

Received 16 February 2007/Returned for modification 10 April 2007/Accepted 27 June 2007

**Collagen degradation is essential for cell migration, proliferation, and differentiation. Two key turnover pathways have been described for collagen: intracellular cathepsin-mediated degradation and pericellular collagenase-mediated degradation. However, the functional relationship between these two pathways is unclear and even controversial. Here we show that intracellular and pericellular collagen turnover pathways have complementary roles in vivo. Individual deficits in intracellular collagen degradation (urokinase plasminogen activator receptor-associated protein/Endo180 ablation) or pericellular collagen degradation (membrane type 1-matrix metalloproteinase ablation) were compatible with development and survival. Their combined deficits, however, synergized to cause postnatal death by severely impairing bone formation. Interestingly, this was mechanistically linked to the proliferative failure and poor survival of cartilage- and bone-forming cells within their collagen-rich microenvironment. These findings have important implications for the use of pharmacological inhibitors of collagenase activity to prevent connective tissue destruction in a variety of diseases.**



The collagens are the most abundant extracellular matrix components in the body and can constitute as much as 90% of the extracellular matrix of a tissue. They consist of three polypeptide chains, each with a single long, uninterrupted section of Gly-X-Y amino acid repeats that are intertwined to produce a superhelix that buries the peptide bonds within the interior of the helix. The fibrillar collagens spontaneously self-associate to form fibrils that range in diameter from 10 to 300 nm, while basement membrane collagens form complicated sheets with both triple-helical and globular motifs (26, 39).

Extensive turnover of collagen takes place during a variety of physiological and pathological tissue-remodeling processes, including development, tissue repair, degenerative connective tissue diseases, and cancer. In this context, collagen turnover serves at least five different functions. It facilitates the physical expansion of a tissue (normal or aberrant), liberates latent growth factors embedded within the extracellular matrix, enables vascular development, subverts the proliferative restrictions imposed on cells by the extracellular matrix, and directly regulates cellular differentiation (5, 22, 30). Inhibition of extracellular matrix degradation, therefore, has long been recognized as an attractive target for therapeutic intervention in a variety of human diseases (1, 6).

Three molecular pathways are known for the turnover of collagen in physiological and pathological tissue-remodeling processes. The best-studied pathway involves a group of secreted or membrane-associated matrix metalloproteinases, the collagenases, that directly cleave collagens within the pericellular or extracellular environment (4, 44). A second, cathepsin K-mediated pathway is specific for osteoclast-mediated bone resorption and takes place in the acidic microenvironment that is created between the ruffled border of the osteoclast and the bone interface (16, 33). The third pathway is intracellular and involves the binding of collagen fibrils to specific cell surface receptors (β1 integrins or urokinase plasminogen activator receptor-associated protein [uPARAP]/Endo180), followed by the cellular uptake, lysosomal delivery, and proteolytic degradation of the acid-denatured collagen by cathepsins (10, 11, 14, 29).

The functional relationship between the intracellular and pericellular collagen degradation pathways is poorly understood and controversial. The cellular uptake of collagen has been reported to be insensitive to metalloproteinase inhibitors (13). However, a recent study proposed that cleavage of collagen by membrane type 1-matrix metalloproteinase (MT1-MMP), the principal mesenchymal cell collagenase (19, 25, 45), was essential for the cellular uptake and lysosomal degradation of collagen by cultured gingival fibroblasts, based on the colocalization of MT1-MMP and actin during collagen phagocytosis (25). This finding contrasts with previous reports of a 40- to 60-fold increase in intracellular collagen in collagen-rich tissues of MT1-MMP-deficient (M−) mice (2, 19). The elucidation of the functional relationship between intracellular and pericellular pathways is important for evaluating the prospects for successfully

* Corresponding author. Mailing address for Thomas H. Bugge: Proteases and Tissue Remodeling Unit, Oral and Pharyngeal Cancer Branch, National Institute of Dental and Craniofacial Research, National Institutes of Health, 30 Convent Drive, Room 211, Bethesda, MD 20892. Phone: (301) 435-1840. Fax: (301) 402-0823. E-mail: thomas.bugge@nih.gov. Mailing address for Kenn Holmbeck: Matrix Metalloproteinases Unit, Craniofacial and Skeletal Diseases Branch, National Institute of Dental and Craniofacial Research, National Institutes of Health, 30 Convent Drive, Room 125, Bethesda, MD 20892. Phone: (301) 496-3922. Fax: (301) 594-1253. E-mail: kenn.holmbeck@nih.gov.

† Supplemental material for this article may be found at http://mcb.asm.org/.

▽ Published ahead of print on 9 July 2007.

using specific inhibitors of pericellular collagenases to prevent extracellular matrix destruction in a variety of diseases (32).

Here we asked whether intracellular and pericellular collagen turnover pathways could act in a complementary manner and, thus, could functionally compensate for each other during the remodeling of a collagen-rich tissue. We focused on bone development because of the high collagen content in cartilage and bone and the well-documented involvement of the pericellular collagenases (19, 23, 38, 45). Specifically, we examined the effect of single and combined null mutations in uPARAP/Endo180, a recently identified cell surface receptor that targets collagen for lysosomal degradation and is highly expressed in developing bone (3, 8, 10–12, 24, 36, 41, 43) (see below), and MT1-MMP, which has a well-established role in collagen turnover during bone formation (19–21, 34, 45). We show that combined deficits in these two collagen turnover pathways have strong synergistic effects on bone formation by directly impairing the survival and proliferation of cells embedded within the collagen-rich bone microenvironment. These data show that the intracellular and pericellular collagen degradation pathways defined by uPARAP/Endo180 and MT1-MMP, respectively, are complementary in vivo, and they identify a novel role for uPARAP/Endo180 in collagen turnover associated with bone formation.

## MATERIALS AND METHODS

**Animals.** The study was carried out in accordance with animal care guidelines from the National Institutes of Health. Mice carrying targeted uPARAP/Endo180 (11) and MT1-MMP (19) alleles in a congenic FVB/N background were interbred to generate littermate offspring with single and combined deficiencies in uPARAP/Endo180 and MT1-MMP. Offspring were weighed every afternoon beginning at 1 day postbirth until weaning or death. At 12 days postbirth, a dough diet was added to cages along with water bottles with long spouts so that the pups could feed on the soft food and reach the water source. Pups were weaned from parents at 21 days postbirth and separated into microisolator cages with a maximum of five weanlings per cage. Cages with M− mice were maintained with the dough diet and long water spouts. Genotyping for the uPARAP/Endo180 endogenous allele was performed with the primers uPARAP E3 3′ (5′-TCTAC ACCATCCAGGGAAACTCAC-3′) and uPARAP E3 5′ (5′-TTAAACTGGTA ACAGCTGTCAGTC-3′). The targeted allele was amplified with uPARAP HPRT (5′-GCAGTTCCCTTTTAAATGCAAATCA-3′) and uPARAP short arm (5′-TCCTACAAATACACGCTGGCGATA-3′). Genotyping for the MT1-MMP endogenous allele was performed with the primers Ex2-Fw (5′-ATGGT TTACAAGTGACAGGCAAGG-3′) and Ex4-revA (5′-GCTCGGCAGAATCA AAGTGG-3′). Genotyping for the MT1-MMP targeted allele was performed with primers KH20 (5′-GTGCGAGGCCAGAGGCCACTTGTGTAGCG-3′) and Int5-rev (5′-AGATGGAGGAGCAGGAATGG-3′).

**Immunohistochemistry.** Slides were deparaffinized in xylene (Mallinckrodt Baker, Phillipsburg, NJ), and the tissue was rehydrated in graded ethanol (EtOH) (100%, 95%, 70%, and $H_2O$). Antigen retrieval was performed using proteinase K (Fisher Scientific, Pittsburgh, PA) treatment (5 mg/ml in 50 mM Tris-HCl [pH 8.0] [Quality Biologicals, Gaithersburg, MD] and 5 mM EDTA [Quality Biologicals]) at 37°C for 10 min and washing in tap water. Endogenous peroxidase activity was quenched by treatment of slides with 1% hydrogen peroxide (Fisher Scientific) in $H_2O$ for 15 min, which were then washed with tap water and transferred to 1× Tris-buffered saline (TBS) (Quality Biologicals) buffer with 0.5% Triton X-100 (Sigma-Aldrich, St. Louis, MO). Slides were incubated overnight at 4°C with purified rabbit polyclonal antibody (2.3 μg/ml) against uPARAP/Endo180, which was generated by immunization with the synthetic peptide N-IPRGVDVREPDIGRQGRLEWV-C as described previously (35), in 1× TBS with 0.25% bovine serum albumin (Sigma-Aldrich). The following day, slides were removed from the cold and incubated for an additional 30 min at room temperature. The slides were washed twice with 0.5% Tween 20 (Bio-Rad Laboratories, Hercules, CA) in 1× TBS. EnVision+ peroxidase anti-mouse antibody (DakoCytomation, Carpinteria, CA) was applied to the slides and incubated for 45 min at room temperature, followed by three washes with TBS–Tween 20 buffer. Dako Nova Red chromogenic substrate (DakoCytomation) was used to visualize expression of uPARAP/Endo180 according to the manufacturer's instructions and incubated for 7 min. The tissue was counterstained in Mayer's hematoxylin (Sigma-Aldrich), blued using 1× TBS, and rinsed in tap water. The slides were mounted with aqueous mounting medium (DakoCytomation) and photographed. For determination of proliferation, mice were injected with 200 μg bromodeoxyuridine (BrdU)/g body weight (Sigma-Aldrich) 2 h prior to euthanasia. Tissues were fixed in 4% paraformaldehyde (PFA) in 1× PBS overnight and embedded in paraffin. Tissue sections (5 μm) were dewaxed in xylene and rehydrated in graded EtOH. Staining for BrdU was performed using a BrdU staining kit (Zymed, South San Francisco, CA) according to the manufacturer's instructions. Quantification was performed by counting the number of positive chondrocytes as a fraction of the total number of chondrocytes in the growth plate, counting a minimum of 500 cells per sample.

Apoptosis analysis was performed by staining with the ApopTag Plus peroxidase in situ apoptosis detection kit (Chemicon International, Temecula, CA) according to the manufacturer's instructions. Slides were counterstained with contrast green (KPL, Gaithersburg, MD). Quantification was performed by counting the number of positive cells per high-power field, with a minimum of three high-power fields analyzed for each sample. Analysis was carried out by an investigator blinded to the genotype of mice.

Collagen type I telopeptides were detected with LF-67 rabbit polyclonal antiserum used at 1:500 (kindly provided by L. Fisher, NIDCR, NIH, Bethesda, MD). Serum from rabbits injected with adjuvant alone was used as a negative control at 1:500. Collagen type II was detected with monoclonal antibody II-II6B3 (1 μg/ml), developed by Thomas F. Linsenmayer and obtained from the Developmental Studies Hybridoma Bank, which was developed under the auspices of the NICHD and is maintained by the University of Iowa, Department of Biological Sciences (Iowa City, IA). Isotype control antibody (EBiosciences, San Diego, CA) (clone P3, immunoglobulin G1 kappa) was used at 1 μg/ml. Immunohistochemistry was performed using the Histomouse-Max kit (Zymed) according to the manufacturer's instructions, and visualization was with diaminobenzidine (Sigma-Aldrich).

**In situ hybridization.** In situ hybridization for collagen types I and II was performed exactly as described previously (20) by using sense and antisense murine collagen type I and II cDNA probes (28, 40). In brief, paraffin sections prepared as described above were dewaxed in xylene, rehydrated through a series of EtOH solutions of decreasing concentrations, treated with 5 μg/ml proteinase K, postfixed in 4% PFA in phosphate-buffered saline (PBS), acetylated in triethanolamine hydrochloride-acetic anhydride, washed in PBS, dehydrated, and air dried. The sections were incubated overnight at 50°C in hybridization buffer containing a single-stranded riboprobe that was radiolabeled with [$^{33}$P]UTP (Perkin-Elmer, Waltham, MA) and complementary sense probes. Collagen type I mRNA was detected using a 2-kb rat cDNA probe, and collagen type II mRNA was detected using a 1.1-kb cDNA probe (both kindly provided by Y. Yamada, NIDCR, NIH, Bethesda, MD). After hybridization, the sections were washed extensively, dehydrated, and air dried. The slides were then dipped in photographic emulsion (Hypercoat LM-1; Amersham Biosciences, Piscataway, NJ) and were exposed for 3 to 5 days at 4°C. After exposure, the slides were developed, counterstained with Mayer's hematoxylin, and photographed using bright-field illumination.

**Hematoxylin and eosin staining.** Tissue was dewaxed in xylene and rehydrated in graded EtOH. Slides were stained with hematoxylin 2 (Richard-Allan Scientific, Kalamazoo, MI) for 3 min, followed by two incubations in tap water. Slides were then incubated in clarifier (Richard-Allan Scientific) for 1 min and rinsed twice in tap water. The slides were blued using bluing reagent (Richard-Allan Scientific) for 1 min and rinsed once in tap water. The slides were then incubated in 95% EtOH and then incubated in eosin (Richard-Allan Scientific) for 40 seconds. The slides were dehydrated through graded EtOH and xylene and mounted with Permount.

**Primary osteoblast and chondrocyte cultures.** Calvarial osteoblasts were isolated from 3-day-old uPARAP/Endo180-sufficient (U+) and uPARAP/Endo180-deficient (U−) littermates. The calvariae were dissected out and placed into alpha-minimal essential medium (Gibco, Carlsbad, CA) containing L-glutamine (Bio-Whittaker, East Rutherford, NJ), 5% fetal bovine serum (FBS) (Gemini Bioproducts, Woodland, CA), and penicillin-streptomycin (Gibco). Calvariae from three mice were pooled for each genotype. Soft tissue from the outside of the calvariae was carefully removed using fine forceps. The calvariae were then cut in half along the midline suture and were placed into 10 ml of 4 mM EDTA (Quality Biological) in a 50-ml glass Erlenmeyer flask in a shaking water bath at 37°C for 10 min. The EDTA was aspirated off, and a second incubation with fresh EDTA was performed. The EDTA was aspirated, and the calvariae were rinsed with 1× PBS. The PBS was aspirated, and the calvariae were incubated at 37°C for 10 min with a digestion solution of 200-U/ml colla-

genase 2 (Worthington Biochemicals, Lakewood, NJ) in 1× PBS with 1.6 μg/ml tosyl-lysyl-chloromethylketone (Calbiochem, La Jolla, CA). The digestion solution was aspirated, and fresh digestion solution was added as before. The second digestion solution was aspirated, and 10 ml of fresh digestion solution was added to the calvariae in the flask and incubated with shaking at 37°C for 15 min. The second digestion solution was passed through a 70-μm nylon cell strainer (BD Falcon, San Jose, CA) into a 50-ml conical tube containing 1× PBS with 5% FBS and placed on ice. This step was repeated twice. After the final digestion, the solution was removed, the calvariae were washed with 1× PBS and the wash was added to the previous digestion solutions. The digestion solution was then spun at 1,000 rpm for 5 min. Cells were seeded onto 10-cm dishes (BD Falcon) at a density of $2 \times 10^4$ cells/ml and grown in alpha-minimal essential medium, L-glutamine, 10% FBS, penicillin-streptomycin, and 55 μM 2-mercaptoethanol (Gibco). For chondrocyte isolation, the cartilaginous part of the rib cage was removed under sterile conditions and incubated at 37°C for 70 min in 1 ml of a solution of 3-mg/ml collagenase 2 in Dulbecco modified Eagle medium (DMEM) (Gibco) in a 50-ml conical tube. After incubation, the tube was vortexed, 1× PBS was added to a total volume of 35 ml, and the tube was shaken vigorously. The bones and cartilage were allowed to settle at the bottom of the tube, and the PBS was aspirated. This step was repeated twice. The cartilage and bone were then incubated overnight at 37°C in 3 ml 0.5-mg/ml collagenase 2 in DMEM with 10% FBS in a six-well plate (Corning Incorporated, Corning, NY). After the overnight digest, the cell solution was transferred to a 50-ml conical tube by filtering through a 70-μm nylon cell strainer. PBS was added, and the suspension was centrifuged at 1,000 rpm for 8 min. This wash step was repeated twice, and the final cell pellet was resuspended in 10% FBS in DMEM with penicillin-streptomycin and L-glutamine and cultured at 37°C at a cell density of $5 \times 10^3$ cells/cm$^2$ for 5 days.

**Collagen degradation assays.** For analysis of pericellular collagenase activity, dishes were coated with a film of reconstituted dried fibrils of either type I collagen, obtained from rat tail tendons as described previously (42), or type II collagen (bovine articular cartilage; US Biological, Swampscott, MA). Type II collagen was dissolved in 0.05 M acetic acid at 4 mg/ml. The solution was brought to neutral pH at a final concentration of 3 mg/ml collagen, and the solution was transferred sequentially through the wells on a 24-well plate, coating the bottom of each well with approximately 30 μl of collagen solution. The collagen was gelled by incubating at 37°C for 1 h and allowed to dry in a laminar flow hood. The dried gel was washed with three changes of water and allowed to dry again. For both collagen types, 25,000 cells were seeded in a 25-μl droplet in the center of each well and allowed to attach for 5 h. The cells were washed and incubated in DMEM with $10^{-9}$ M interleukin-1β (Peprotech, Rocky Hill, NJ) and $10^{-8}$ M tumor necrosis factor alpha (Peprotech) for 1 week. The cells were removed with 1% Triton X-100 (Sigma-Aldrich) in trypsin-EDTA (Invitrogen), and the collagen was stained with Coomassie blue (Sigma-Aldrich). The collagen film was photographed on an inverted Nikon Axiophot microscope with a 10× objective. For intracellular collagen degradation, acid-extracted rat tail tendon collagen was conjugated to fluorescein as described previously (18). The gel was then washed extensively with borate buffer at room temperature, the borate was washed out with water, and the labeled collagen was dissolved in 20 mM HCl at 4°C. Chondrocytes or osteoblasts isolated from uPARAP/Endo180-sufficient and -deficient mice were seeded onto glass coverslips coated with polylysine (Sigma-Aldrich) in 24-well tissue culture plates (Corning Incorporated) at a density of $1 \times 10^4$ cells/well in their appropriate growth media (see above). Cells were grown for 48 h and then washed in serum-free medium. E-64d (Calbiochem) was added to a final concentration of 20 μM and left for 1 h in serum-free conditions. The medium was changed to fresh serum-free medium with E-64d after 1 h, and collagen type I fibrils were added to a final concentration of 25 μg/ml and left for 8 h. LysoTracker-red (Molecular Probes, Eugene, OR) (50 nM final concentration) was added to cells and left for 90 min. Cells were washed with 1× PBS and fixed in 4% PFA, 1× PBS, and 0.05% Triton X-100 (Sigma-Aldrich) for 20 min in the dark. The cells were washed with PBS, incubated for 20 min at room temperature in 100 mM glycine (Invitrogen) in 1× PBS, and washed in PBS and then in water. Nuclei were stained with Hoechst (1/10,000) (Molecular Probes) for 5 min and washed with PBS. Coverslips were mounted onto glass slides using Vectashield (Vector Laboratories, Burlingame, CA) to prevent fading, according to the manufacturer's instructions. Confocal images were collected on a Leica TCS SP2 confocal system using a DM-RE-7 upright microscope and a 63×, 1.32-NA objective in the NIDCR Imaging Facility. Projection images from 0.15-μm Z-stacks were made using the Leica LCS software.

**Cartilage and bone staining.** Mice were euthanized. The skin was removed, the abdominal cavity was opened, and the pups were fixed in 95% EtOH for a minimum of 4 days. Any remaining skin and fat from mice were carefully dissected off of the carcasses, and the internal organs were removed. The remaining adipose tissue was dissolved by incubation in acetone (Mallinckrodt) for 48 h. Cartilage and bone were stained for 1 week in 1 volume 0.3% alcian blue in $H_2O$, 1 volume 0.1% alizarin red in $H_2O$ (both Sigma-Aldrich), 1 volume glacial acetic, acid and 17 volumes of 75% EtOH. The samples were rinsed in water, and tissue was cleared in a solution of 1% KOH with frequent changes of solution, for approximately 1 to 2 weeks depending on age of mice. The KOH solution was removed, and samples were incubated with increasing concentrations of glycerol (10% to 50%) in water over several days. Samples were photographed using a Kodak DCS 760 camera.

**X-ray analysis.** Freshly euthanized pups were positioned on a Plexiglas sheet in a Faxitron MX-20 (X-ray Corporation, Wheeling, IL), and Kodak X-OMAT V film was used to image mice by exposure for 900 s at 30 kV at a magnification of either 1.5×, 3×, or 4×, depending on the age of the mice. Autoradiographs were scanned with an Epson expression 1680 at a setting of 900 dpi using Adobe Photoshop. Bone length was measured using the measurement tool in ImageJ by an investigator blinded to mouse genotype.

**Determination of bone mineral density by computer-assisted tomography.** Pups were sacrificed using a lethal intraperitoneal injection of xylazine, ketamine, and azepromazine. The skin was removed, and the body cavity was exposed. Pups were fixed and stored in 70% EtOH. To image the calvarium, the top of the skull was cut off, the brain was removed, and bone tissue was trimmed. To image femurs, the legs were cut off at the hip and femur, and surrounding soft tissue was carefully dissected. The day prior to imaging, tissue was transferred to 1× PBS. For imaging, tissues were wrapped in a sponge soaked in 1× PBS and placed in the specimen holder. Tissues were imaged at 14-μm resolution (80 kV, 80 μA) using an Explore Locus SP CT-scanner (General Electric Healthcare, Fairfield, CT). Image analysis and determination of bone mineral density and cortical bone thickness were performed using MicroView 2.1 software (General Electric Healthcare).

**Determination of osteoblast activity.** Pups were injected intraperitoneally with calcein (Sigma-Aldrich) at a dose of 25 mg/kg in 2% $NaHCO_3$ at 4 days postbirth. The pups were sacrificed 2 days later, and heads were removed and fixed in 70% EtOH overnight at room temperature in the dark. The calvarium was dissected from the remainder of the skull, the brain was removed, and the calvarium was visualized under UV light. Digital images were obtained using the AlphaImager system (Alpha Innotech, San Leandro, CA). The digital images were then analyzed using ImageJ software. For presentation, the images were pseudocolored in ImageJ using the "fire/ice" setting. Quantitation was done using the "ROI manager and measurement" tool in ImageJ.

## RESULTS

**uPARAP/Endo180 is expressed in developing bone and mediates the cellular uptake and lysosomal degradation of collagen by chondrocytes and osteoblasts.** Immunohistochemical analysis of wild-type mouse pups showed that uPARAP/Endo180 was abundantly expressed in bone-forming tissues (Fig. 1). This included both long bones undergoing endochondral ossification and calvarial bones undergoing intramembranous ossification. This expression pattern was in agreement with previous uPARAP/Endo180 mRNA localization studies (12, 43). Specifically, the collagen internalization receptor was expressed by resting, reserve, and proliferating zone chondrocytes and by osteoblasts/osteocytes but was absent from other cell populations within developing bones, such as endothelial cells and hypertrophic chondrocytes (Fig. 1A, C, and E and data not shown). The specificity of the immunohistochemical detection was verified by the absence of staining of uPARAP/Endo180-deficient bones (Fig. 1B, D, and F). As reported previously for uPARAP/Endo180 mRNA (12), uPARAP/Endo180 protein expression largely was absent from other tissues of newborn animals, suggesting a specific involvement of the collagen internalization receptor in hard tissue formation during perinatal and early postnatal development.

To determine the functional significance of uPARAP/Endo180 expression in bone-forming tissues, we explanted chondrocytes and osteoblasts from newborn U+ and U− mice

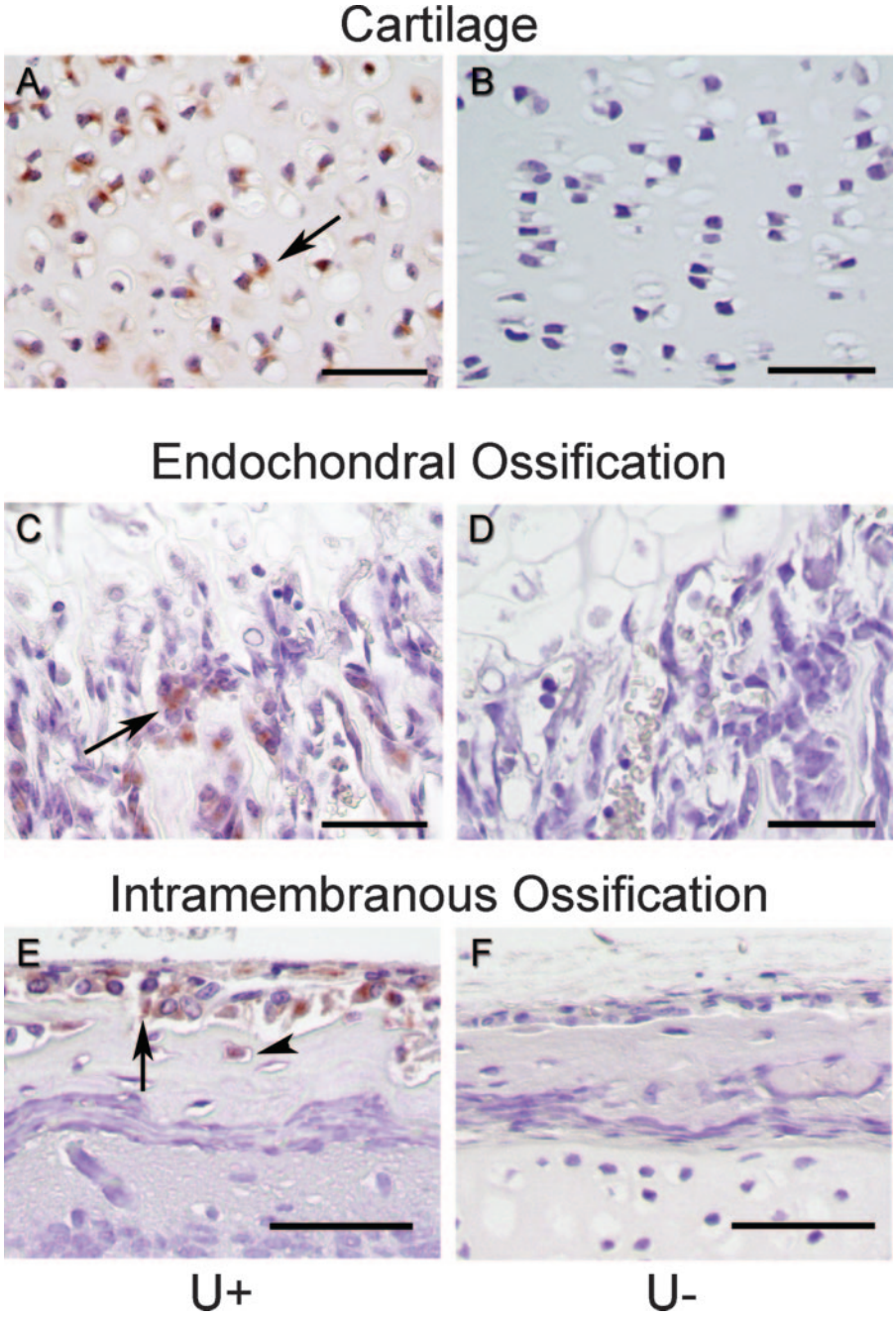


FIG. 1. uPARAP/Endo180 is expressed in developing bones. uPARAP/Endo180 immunohistochemical staining in proliferative zone chondrocytes of the epiphyseal growth plate of the femur (A and B), primary spongiosa of the femur (C and D), and calvarial intramembranous ossification site (E and F) from 6-day-old U+ (A, C, and E) and U− (B, D, and F) pups is shown. uPARAP/Endo180 is prominently expressed in proliferative zone chondrocytes (arrow in panel A), in osteoblasts engaged in endochondral ossification (arrow in panel C), in osteoblasts engaged in intramembranous ossification (arrow in panel E), and in osteocytes (arrowhead in panel E). The specificity of the immunohistochemistry is indicated by the absence of staining of corresponding U− tissues (B, D, and F). Bars, 50 μm.

into primary cultures and determined their capacity to internalize and lysosomally degrade collagen, using a recently developed procedure (8, 24). Fluorescein-conjugated, acid-extracted native fibrillar collagen was added to the explants, and the fate of the labeled collagen was revealed by confocal fluorescence microscopy in the presence of the cysteine protease inhibitor E-64d, which blocks lysosomal degradation of collagen. After 4 hours, most of the labeled collagen added to U+ chondrocyte explants was located in distinct extracellular structures (data not shown). After 8 hours, however, little extracellular collagen was observed, and most of the collagen was found in cytoplasmic vesicular structures within the chondrocytes (Fig. 2A and D). These collagen-containing vesicular structures frequently were positive for LysoTracker, a specific

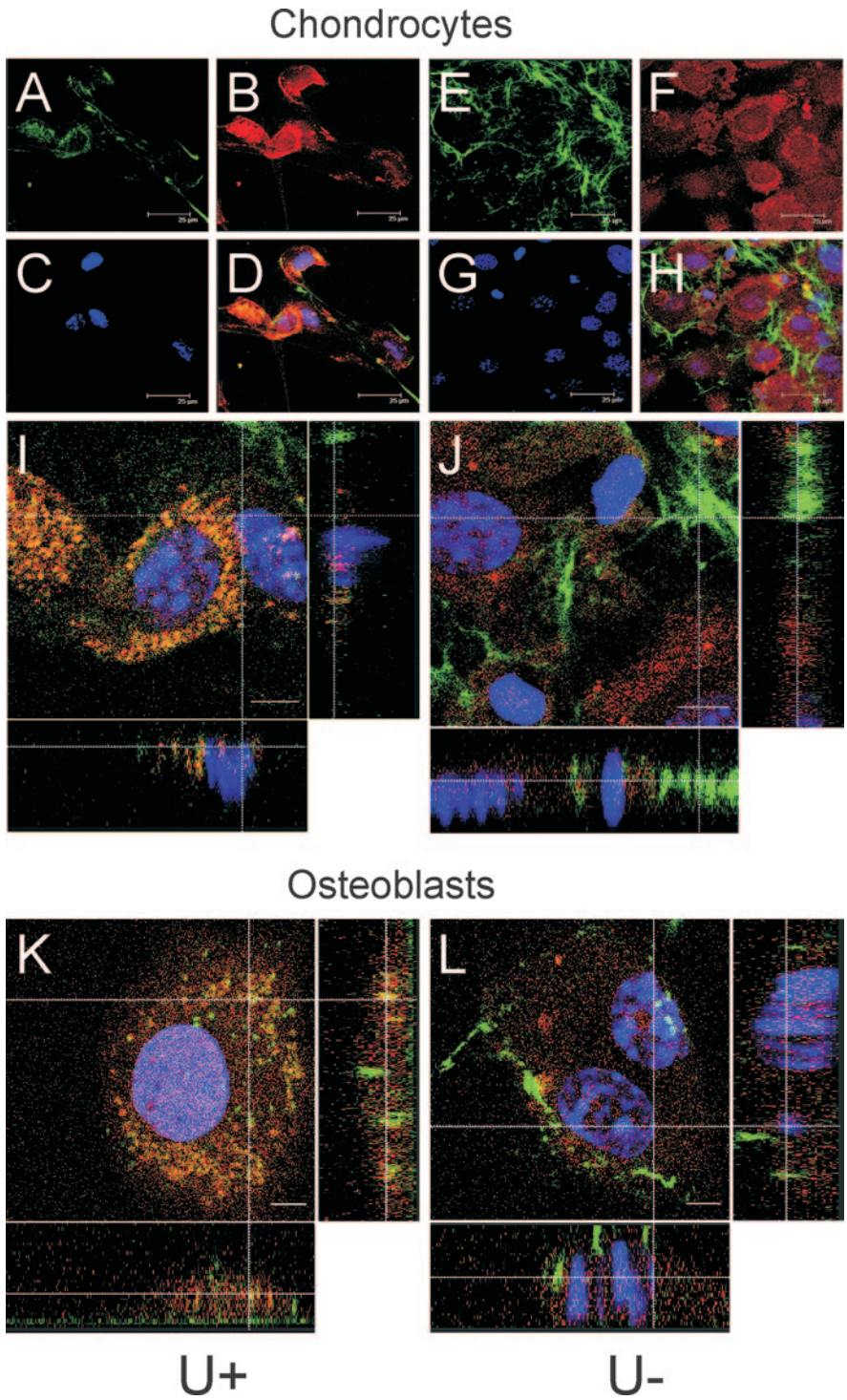


FIG. 2. uPARAP/Endo180 mediates cellular uptake and lysosomal degradation of collagen by both chondrocytes and osteoblasts. U+ (A to D, I, and K) and U− (E to H, J, and L) chondrocytes (A to J) and osteoblasts (K and L) were explanted to primary cultures. Fluorescein-conjugated, acid-extracted fibrillar rat tail tendon collagen (green) was added to the cultures and left for 8 h in the presence of the lysosomal cysteine protease inhibitor E-64d. The cells were stained with LysoTracker (red) for the visualization of lysosomes and with Hoechst stain (blue) for the visualization of nuclei and examined by confocal fluorescence microscopy. (A to H) Maximal averages of 0.15-μm z-stacks from bidirectional sequential acquisition of collagen (A and E), lysosomes (B and F), and nuclei (C and G) and merged images of panels A to C and panels E to G (D and H, respectively). (I and J) Merged images of a single 0.15-μm z-stack. The bottom of each image in panels I to L shows a stack of the x-z axis indicated by horizontal line, and right side of each image in panels I to L shows a stack of the y-z axis indicated by the vertical line. In U+ chondrocyte and osteoblast cultures, collagen is predominantly located in intracellular vesicular structures that frequently are positive for LysoTracker (yellow color in panels D, I, and K). In U−chondrocyte and osteoblast cultures, collagen is predominantly located in extracellular fiber-like structures that form a cast around cells (E, H, J, and L). Bars, 25 μm (A to H) and 7.5 μm (I to L).

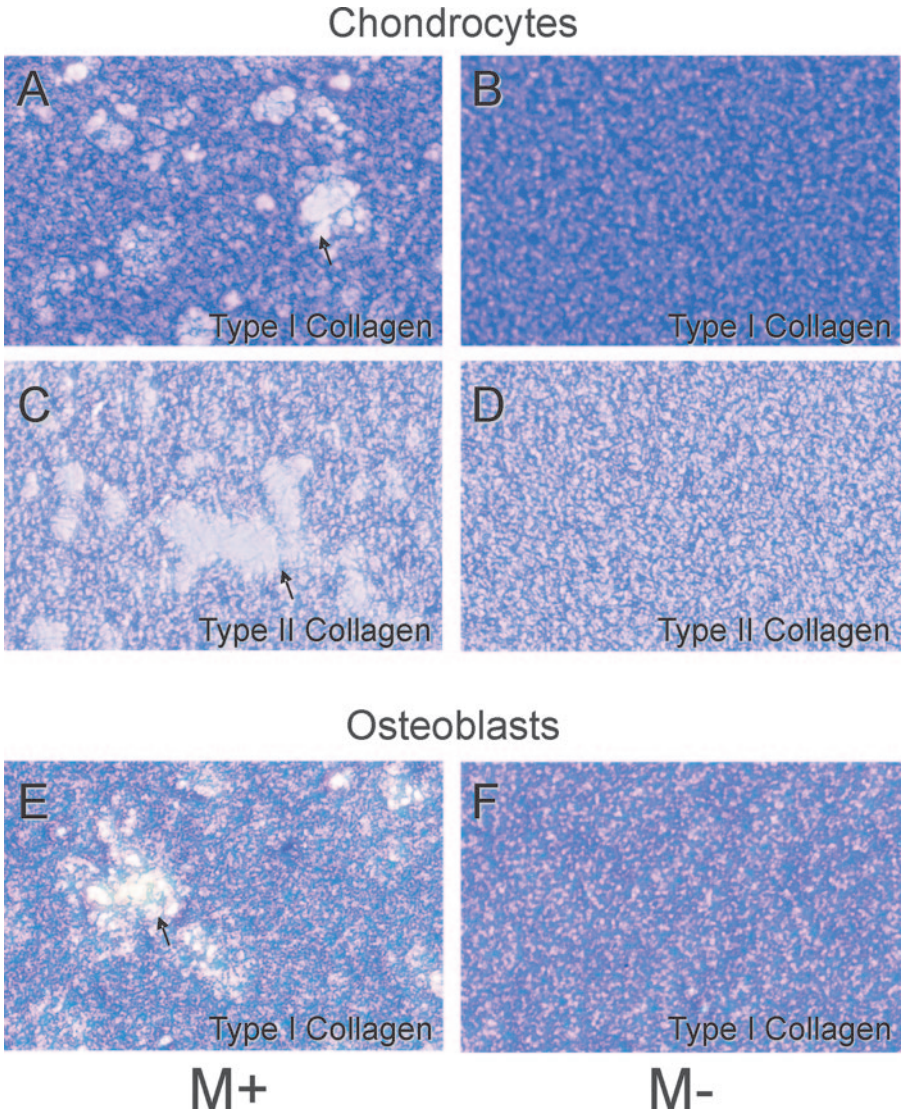


FIG. 3. MT1-MMP mediates pericellular degradation of collagen by both chondrocytes and osteoblasts. M+ (A, C, and E) and M− (B, D, and F) chondrocytes (A to D) and osteoblasts (E and F) were placed on a layer of fibrillar type I (A, B, E, and F) or type II (C and D) collagen. Collagenolytic activity was induced with interleukin-1β and tumor necrosis factor alpha, and zones of lysis were visualized by Coomassie brilliant blue staining after removal of cells. M+ chondrocytes and osteoblasts display collagenolytic activity, which is completely abrogated in M− chondrocytes and osteoblasts.

marker for lysosomes, showing that internalized collagen was being targeted for lysosomal degradation (Fig. 2D and I). In marked contrast, collagen added to U− chondrocytes organized almost exclusively in fiber-like structures that formed a conspicuous cast around cells (Fig. 2E and H), and little uptake of collagen into cytoplasmic vesicles was observed (Fig. 2H and J). Identical results were obtained when collagen uptake was studied in U+ and U− osteoblast cultures (Fig. 2K and L and data not shown). Taken together, these data show that the uPARAP/Endo180-dependent intracellular collagen turnover pathway is operative on both chondrocytes and osteoblasts. To determine if MT1-MMP-dependent collagenolytic activity was required for uPARAP/Endo180-mediated collagen internalization, we performed the identical collagen internalization experiments with MT1-MMP-sufficient (M+) and -deficient (M−) chondrocytes and osteoblasts. These experiments revealed that the two cell types retained their ability to internalize and lysosomally degrade collagen in the absence of MT1-MMP (see Fig. S1 in the supplemental material).

**MT1-MMP is required for pericellular collagen degradation by both chondrocytes and osteoblasts.** The requirement of MT1-MMP for pericellular degradation of collagen by primary chondrocytes and osteoblasts was determined next. M+ and M− chondrocytes and osteoblasts were plated on a layer of fibrillar collagen. The capacities of the two cell types to degrade the collagen were determined after cytokine induction of collagenolytic activity. Both M+ chondrocytes and M+ osteoblasts degraded their respective collagen substrates as shown by the distinct zones of lysis beneath the cells (Fig. 3A, C, and E). In sharp contrast, no collagen-degrading activity was ob-

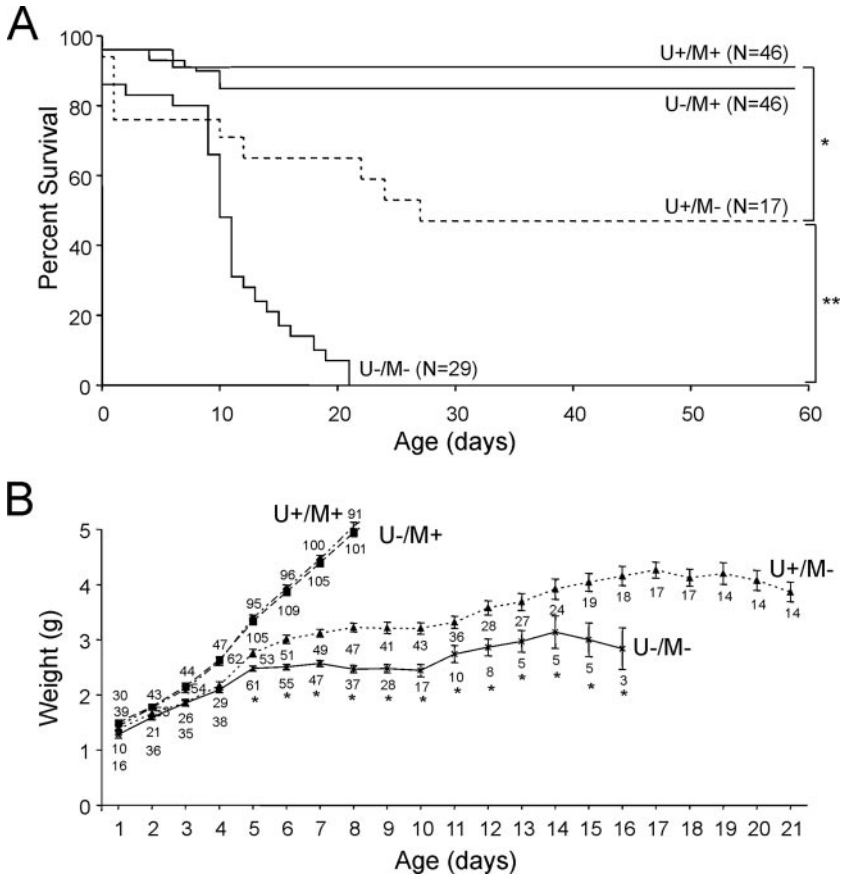


FIG. 4. Combined loss of uPARAP/Endo180 and MT1-MMP causes postnatal death. FVB mice with targeted uPARAP/Endo180 and MT1-MMP alleles were interbred to generate U+/M+, U−/M+, U+/M−, and U−/M− littermate offspring. (A) Sixty-day survival of a prospective cohort initially consisting of 46 U+/M+, 46 U−/M+, 17 U+/M−, and 29 U−/M− mice. All U−/M− mice perished before day 21, while the 60-day survival of U+/M+ mice was 91%, survival of U−/M+ mice was 85%, and survival of U+/M− mice was 47%. *, $P < 0.0012$; **, $P < 0.007$ (Mann-Whitney U test, two tailed). (B) Weight gain of newborn U+/M+ (open squares), U−/M+ (solid squares), U+/M− (triangles), and U−/M− mice (stars) followed for up to 21 days. Numbers above or below symbols indicate the number of mice included in each weight measurement. The weight of U−/M− mice is identical to that of U+/M− mice at days 1 to 4 but 10 to 32% lower than that of U+/M− mice at days 5 to 16. Data are shown as means ± standard errors of the means. *, $P < 0.05$ for U−/M− relative to U+/M− mice (Student's *t* test, two tailed).

served in either cultured M− chondrocytes or M− osteoblasts (Fig. 3B, D, and F). These data show that pericellular collagen degradation by these cells is MT1-MMP dependent. uPARAP/Endo180 is a cellular receptor for collagen and could potentially contribute to MT1-MMP-mediated pericellular collagen degradation (3, 11). To investigate this possibility, the capacities of cytokine-stimulated U+ and U− chondrocytes and osteoblasts to degrade fibrillar collagen were determined. No detectable difference in pericellular collagenolysis was observed with either chondrocytes or osteoblasts, indicating that MT1-MMP operates independently of uPARAP/Endo180 (see Fig. S2 in the supplemental material).

**Postnatal death caused by combined deficits in intracellular and pericellular collagen degradation pathways.** Because of the engagement of both uPARAP/Endo180 and MT1-MMP in collagen turnover, the conspicuous similarity of the expression patterns of the two molecules in bone-forming tissue (see above) (19–21, 45), the fundamentally different mechanisms of collagen turnover (intracellular versus pericellular), and the marked accumulation of intracellular collagen in bone-forming cells of M− mice (2, 19), we hypothesized that the collagen turnover pathways defined by the two molecules could act in a complementary manner within the bone microenvironment. If this was true, combined uPARAP/Endo180 and MT1-MMP deficiencies would be predicted to have a more severe effect on bone formation than an individual deficiency in either uPARAP/Endo180 or MT1-MMP. To test this proposition, we interbred FVB mice with targeted uPARAP/Endo180 and MT1-MMP alleles to generate mice with single and combined deficiencies in each molecule. Doubly deficient (U−/M−) offspring were born with the expected Mendelian frequency, showing that a combined deficit in both collagen turnover pathways is compatible with prenatal development (data not shown). As shown previously (10, 11), mice tolerated the absence of uPARAP/Endo180. Thus, the postnatal survival of U− mice was not significantly different from that of U+ littermates in a prospective cohort that was followed for 60 days (Fig. 4A). As also reported previously (19), loss of MT1-MMP impaired postnatal survival, with approximately half of the M− mice perishing within 60 days of birth (Fig. 4A). Interestingly,

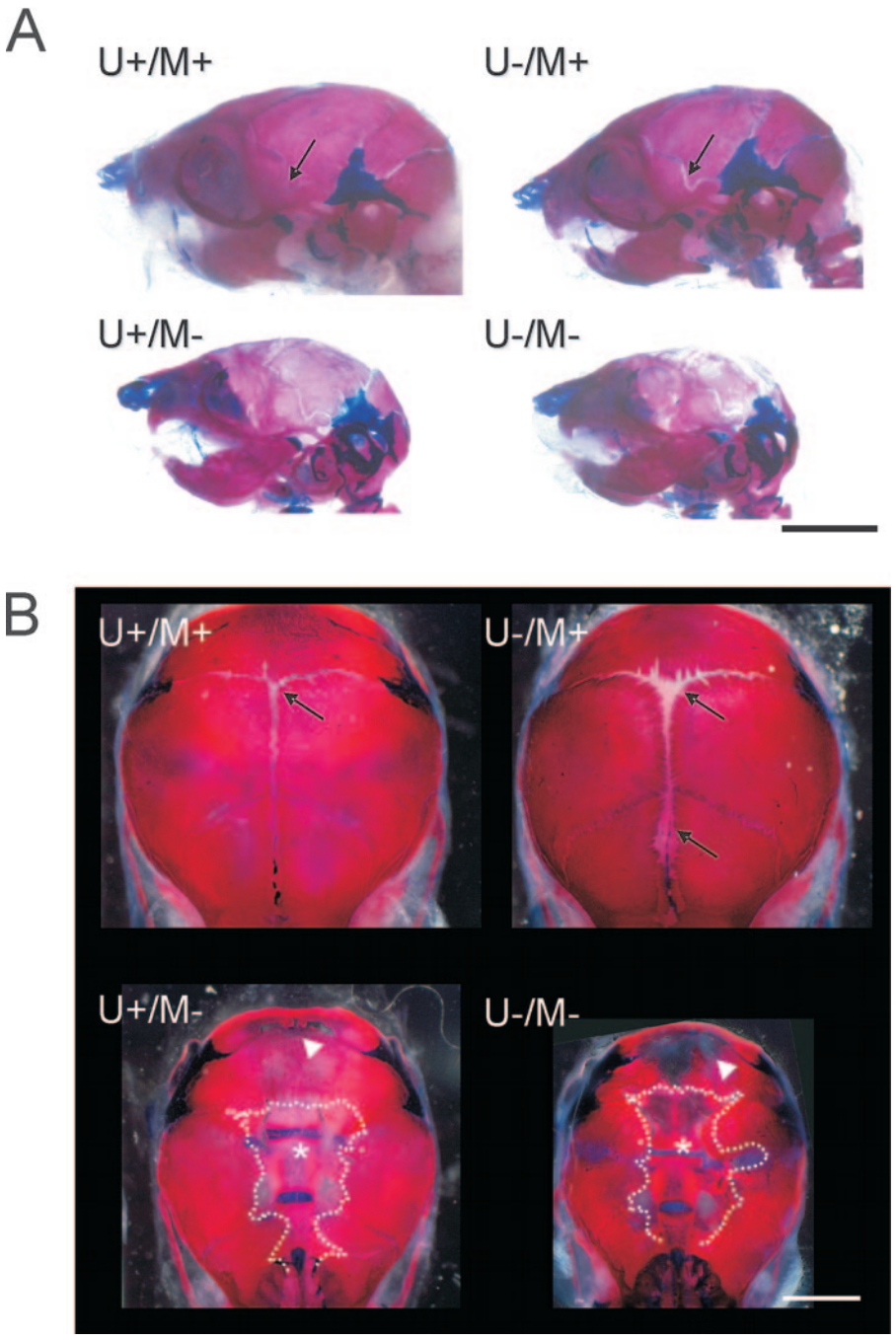


FIG. 5. Combined uPARAP/Endo180 and MT1-MMP deficiency exacerbates craniofacial deficiencies in mice with single uPARAP/Endo180 or MT1-MMP deficiency. (A) Alcian Blue/Alizarin Red staining of the cranium of 8-day-old U+/M+, U−/M+, U+/M−, and U−/M− mice. Widened cranial sutures and fontanels in U−/M+ compared to U+/M+ mice are seen (arrows). (B) Top view of the calvariae of 8-day-old U+/M+, U−/M+, U+/M−, and U−/M− mice. Widened cranial sutures and fontanels in U−/M+ compared to U+/M+ mice (arrows) and diminished calvarial bone in U−/M− compared to U+/M− mice (dark spaces, arrowheads) are seen. Dotted lines in panel B demark the edges of the U+/M− and U−/M− calvariae, and the underlying cranial bones exposed by the absence of fontanel closure are indicated with asterisks. Bars, 4 mm (A) and 2 mm (B).

however, the superposition of uPARAP/Endo180 and MT1-MMP deficiencies caused uniform, early postnatal lethality, indicating that uPARAP/Endo180 and MT1-MMP acted in a complementary rather than an interdependent manner. Seventy percent of the U−/M− pups perished within 11 days of birth, and all U−/M− pups died prior to weaning at 21 days of age. U−/M− pups appeared outwardly normal at birth (data not shown), and their body weight was not significantly different from that of U−, M−, or U+/M+ littermates (Fig. 4B). However, between days 4 and 5, the U−/M− pups began to

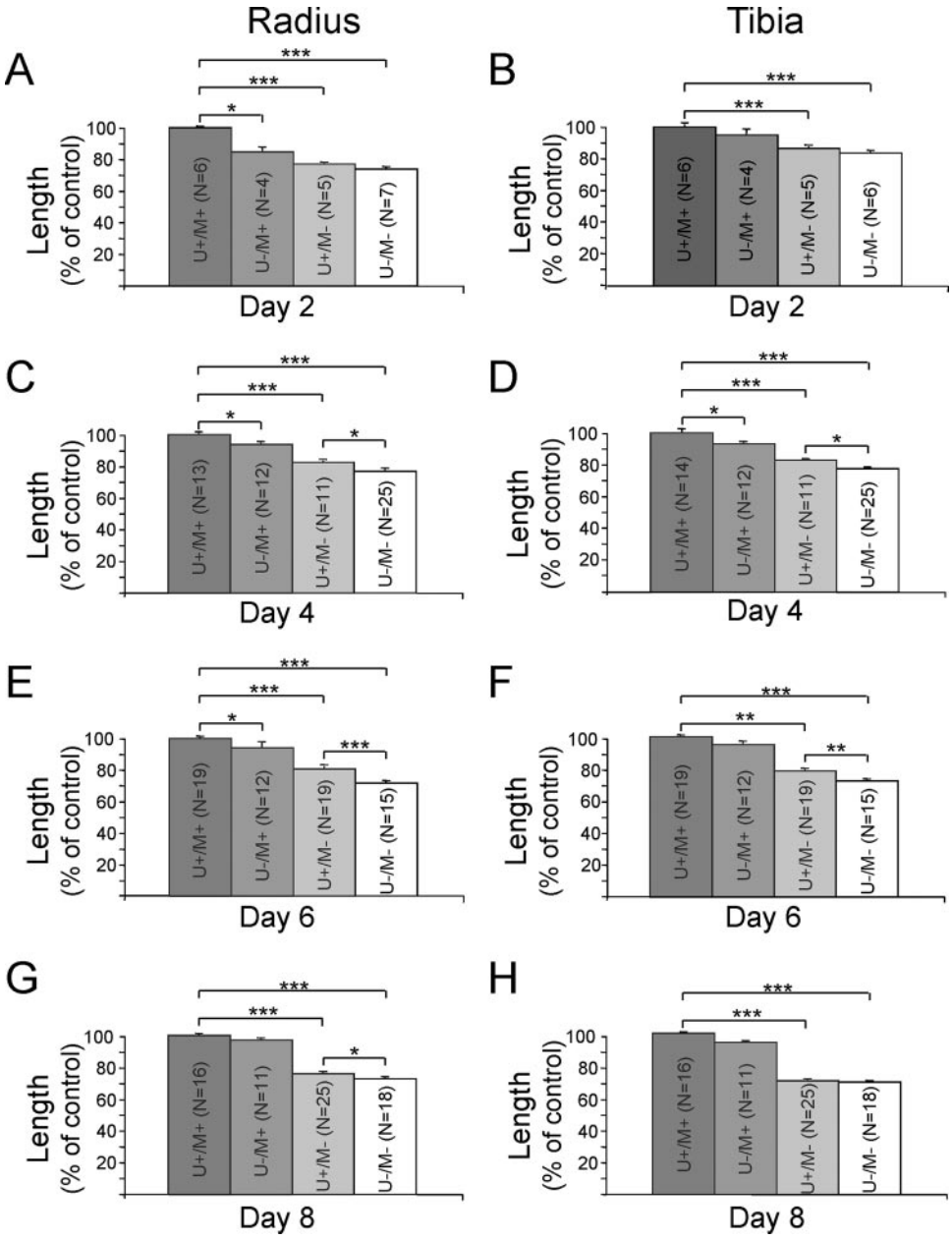


FIG. 6. Impairment of long bone length after combined uPARAP/Endo180 and MT1-MMP deletion. Lengths of radii (A, C, E, and G) and tibias (B, D, F, and H) of U+/M+, U−/M+, U+/M−, and U−/M− pups at 2 (A and B), 4 (C and D), 6 (E and F), and 8 (G and H) days after birth, as determined by X-ray analysis, are shown. Data are shown as means ± standard errors of the means. *, $P < 0.05$; **, $P < 0.01$; ***, $P < 0.001$ (Student's *t* test, two tailed). N, number of mice included in each measurement.

display a significant growth retardation compared to both U− and M− mice. Interestingly, the time of onset of growth retardation of the U−/M− pups coincided with the time of onset of a significant growth retardation of M− pups relative to M+ pups due to their collagenolytic deficit. Taken together, these data show that combined uPARAP/Endo180 and MT1-MMP deficiencies, but not a single deficiency of either molecule, is incompatible with postnatal survival.

**Combined deficits in intracellular and pericellular collagen degradation pathways inhibit bone formation.** As expected from the restriction of uPARAP/Endo180 expression to hard tissues, a histological survey of soft tissues of pups aged 2 to 8 days did not reveal any differences between U+/M+, U−, M−, and U−/M− offspring (data not shown). However, combined deficits in the collagen turnover pathways defined by the two molecules had striking synergistic effects on bone formation. An initial qualitative inspection of Alcian Blue/Alizarin Red-stained long bones (data not shown) and cranium (Fig. 5) indicated a diminished cranial bone formation, and reduced long bone length and ossification in mice with combined deficits in the two collagen internalization pathways compared to mice with a single deficiency in each pathway. To analyze long

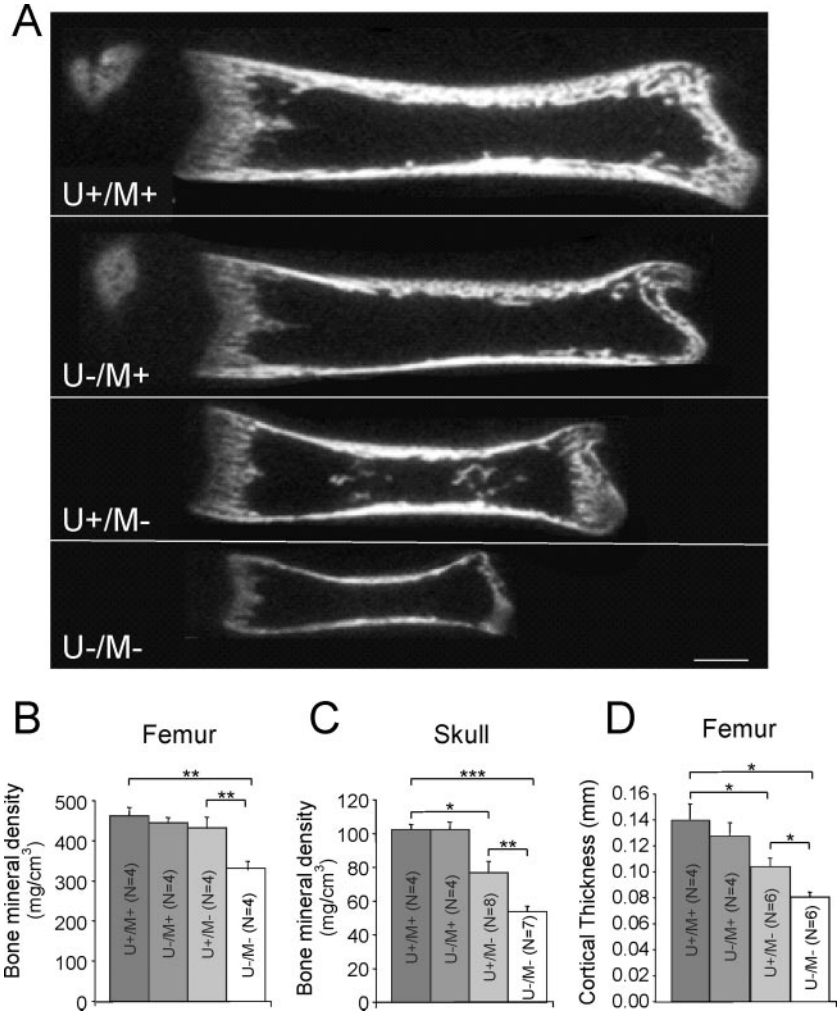


FIG. 7. Synergistic impairment of bone mineralization caused by simultaneous uPARAP/Endo180 and MT1-MMP deletion. (A) Representative example of computerized tomography analysis used for determination of the bone mineral densities of the femurs of U+/M+, U−/M+, U+/M−, and U−/M− pups 8 days after birth. (B to D) Bone mineral densities of femurs (B) and calvariae (C) and cortical thicknesses of femurs (D) of 8-day-old U+/M+, U−/M+, U+/M−, and U−/M− pups as determined by computerized tomography. Data are shown as means ± standard errors of the means. *, $P < 0.05$; **, $P < 0.01$; ***, $P < 0.001$ (Student's $t$ test, two tailed). N, number of mice included in each measurement.

bone formation quantitatively, X-ray analysis of pups at various times after birth was performed. This analysis revealed a significant reduction of the length of the long bones of both U− and M− pups, which was appreciable as early as day 2 after birth, with loss of MT1-MMP generally having a more pronounced effect than loss of uPARAP/Endo180 (Fig. 6). Single deficiency in either uPARAP/Endo180 or MT1-MMP reduced long bone (radius and tibia) length at days 2 to 6 after birth by 6 to 8% and 15 to 22%, respectively. Combined uPARAP/Endo180 and MT1-MMP deficiencies resulted in a more severe reduction in long bone length than an individual deficiency in each molecule, with a 19 to 28% reduction of long bone length of U−/M− pups compared to U+/M+ pups (Fig. 6).

In addition to bone length, the combined deficiencies in uPARAP/Endo180 and MT1-MMP had a strong synergistic effect on the ossification of bones. Computer-assisted tomography of long bones revealed only small reductions in bone mineral density of U− and M− mice (4 and 8%, respectively) (Fig. 7A and B). In contrast, the combined deficiencies of uPARAP/Endo180 and MT1-MMP reduced the mineral density of long bones by as much as 30% (Fig. 7A and B) and caused a 42% reduction in cortical bone thickness (Fig. 7D).

The same synergistic effect of combined deficiencies in uPARAP/Endo180 and MT1-MMP was observed on calvarial bone formation, with 0, 25, and 47% reductions in the bone mineral densities of U−, M−, and U−/M− pups, respectively (Fig. 7C).

We next performed calcein incorporation assays to determine if the synergistic reduction in ossification of bones in combined U−/M− pups was caused by a diminution of the rate of bone deposition by osteoblasts. U+/M+, U−, M−, and U−/M− littermate pups were injected with calcein, and the incorporation of this calcium fluorophor into calvarial bones was quantified after 48 h (Fig. 8). In accordance with the effect on bone mineral density, a single deficiency in either uPARAP/Endo180 or MT1-MMP had a more modest

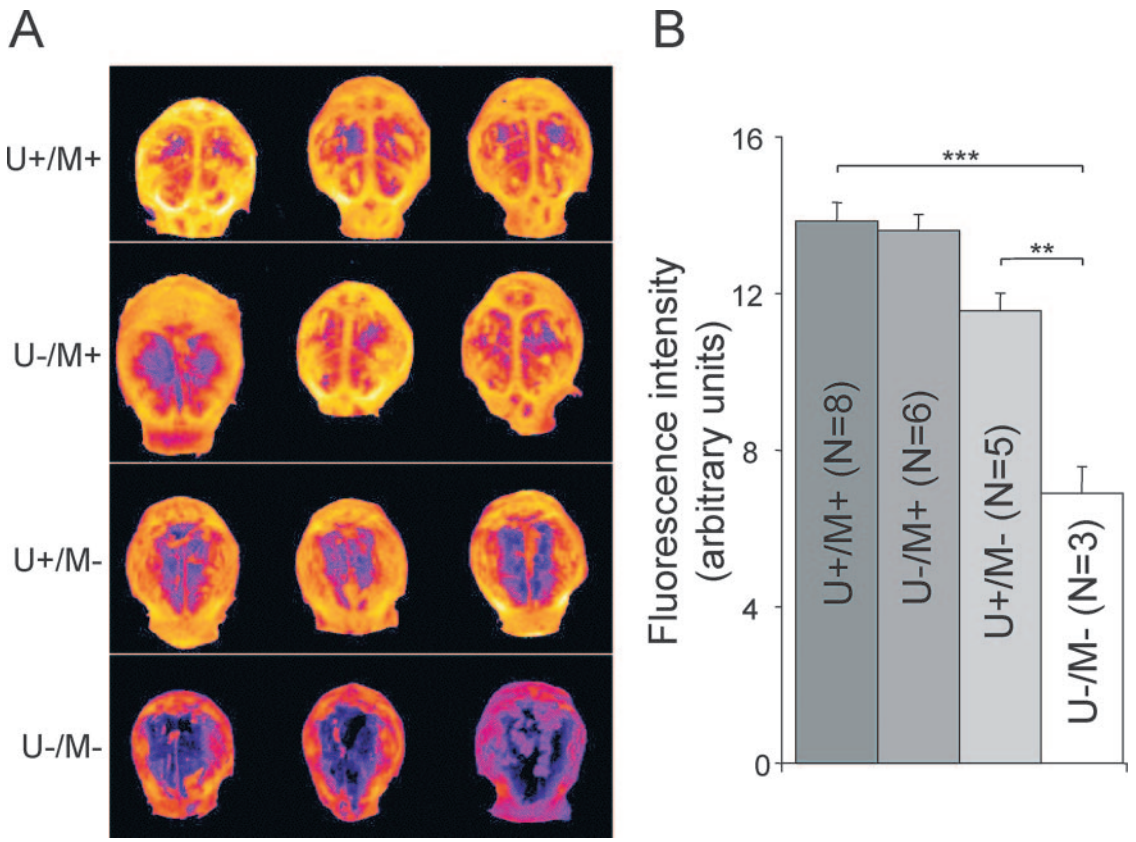


FIG. 8. Synergistic impairment of bone synthesis by combined uPARAP/Endo180 and MT1-MMP deficiency. (A) Representative examples of calcein incorporation into the calvarium of 6-day-old U+/M+, U−/M+, U+/M−, and U−/M− pups are shown. Yellow color shows areas of high osteoblast activity and blue color those of low osteoblast activity. (B) Quantitation of calcein incorporation into the calvarium of U+/M+, U−/M+, U+/M−, and U−/M− mice. Data are shown as means ± standard errors of the means. **, $P < 0.01$; ***, $P < 0.001$ (Student's $t$ test, two tailed). N, number of calvariae included in each measurement.

effect on osteoblast activity (4 and 20% reduction, respectively) than their combined deficiencies (50% reduction of osteoblast activity).

**Loss of bone formation in uPARAP/Endo180 and MT1-MMP doubly deficient mice is mechanistically linked to proliferative failure and poor survival of cells in the bone microenvironment.** Cartilage and bone are both among the most collagen-rich tissues in the body. In situ hybridization and immunohistochemistry of long bones showed that chondrocytes of mice of all genotypes retained the overall ability to synthesize and deposit a collagen type II-rich cartilage matrix, as well as a type I-rich bone matrix during endochondral ossification (see Fig. S3 and Fig. S4 in the supplemental material). Recent studies have shown that pericellular collagen turnover is a critical determinant of the proliferation of cells within a collagen-rich microenvironment (22). However, the effect of intracellular collagen degradation on cell proliferation and the ability of the intracellular pathway to compensate for proliferative deficits caused by loss of pericellular collagenolysis are unexplored. We therefore determined if the synergistic effect of combined uPARAP/Endo180 and MT1-MMP deficiencies on bone development was mechanistically linked to a diminution of cell proliferation within the bone microenvironment. For this purpose, chondrocyte proliferation within the proliferative zone of the epiphyseal growth plate of the long bones was determined by BrdU incorporation (Fig. 9A). Enumeration of BrdU-incorporating cells showed 14 and 23% reductions in the rate of cell proliferation in the proliferative zones of the tibial epiphyseal growth plates of U− and M− pups, respectively (Fig. 9B and C). Interestingly, however, a strong synergistic impairment of cell proliferation resulted from the combined deficit of uPARAP/Endo180 and MT1-MMP, with cell proliferation rates being reduced by as much as 58% in the tibial chondyle of U−/M− pups. Similar results were obtained after enumerating cell proliferation in the femoral chondyle (data not shown).

Strong synergistic effects of combined uPARAP/Endo180 and MT1-MMP deficiencies were observed not only on cell proliferation but also on apoptosis of cells within the primary spongiosa (Fig. 9A). In the primary spongiosa of the tibia, single uPARAP/Endo180 or MT1-MMP deficiency caused 10 and 81% increases in apoptosis, respectively, while combined deficiencies caused a 154% increase in apoptosis (Fig. 9D and E). Similarly, in the primary spongiosa of the femur, single deficiency of either uPARAP/Endo180 or MT1-MMP did not significantly increase apoptotic rates, but combined deficiencies of the two molecules caused a 112% increase in apoptosis (data not shown). Taken together, these data show that both intracellular collagen

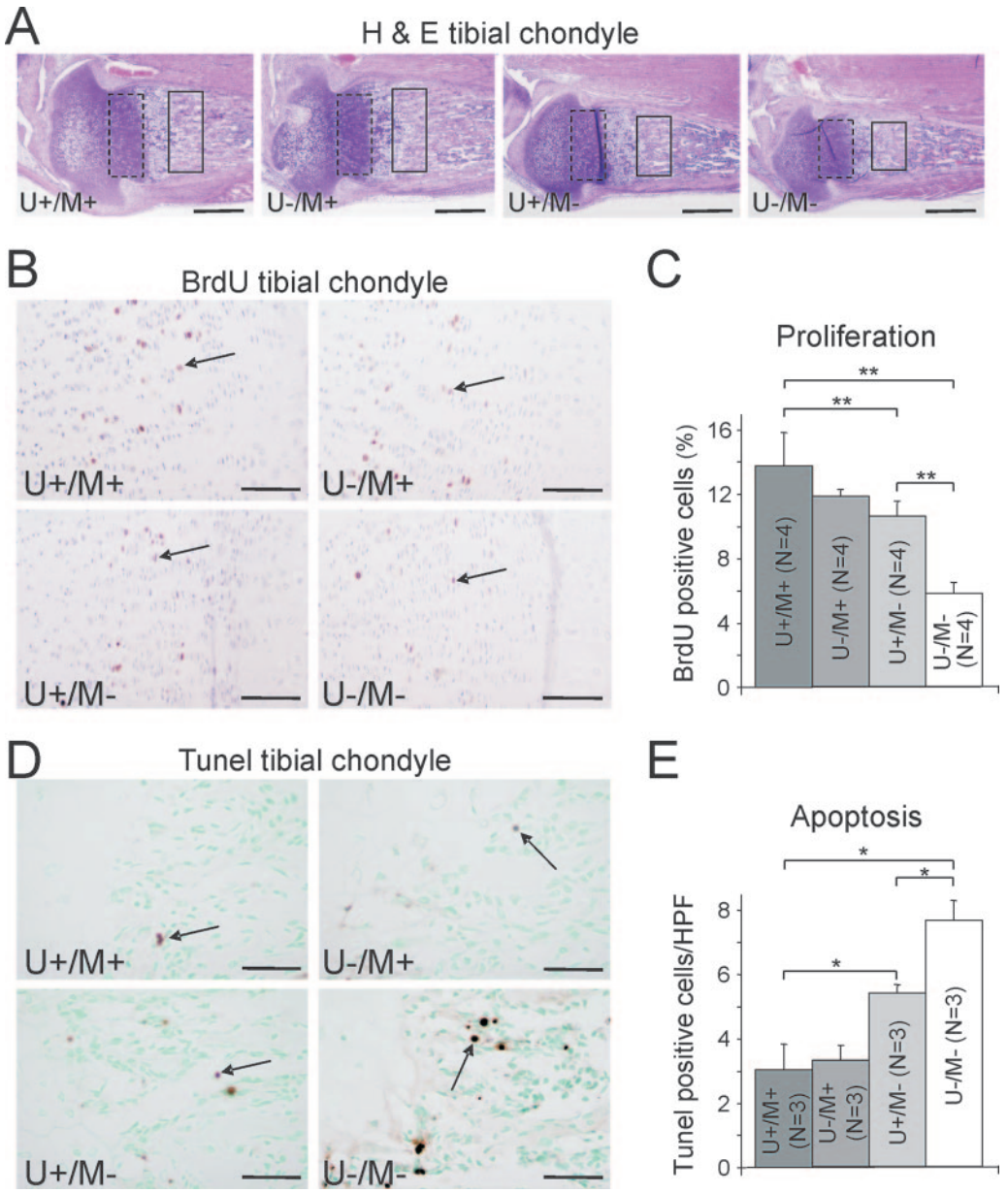


FIG. 9. Impaired bone formation in U−/M− mice is mechanistically linked to reduced cell proliferation and survival. (A) Hematoxylin and eosin staining of the tibias of 6-day-old U+/M+, U−/M+, U+/M−, and U−/M− pups. Cell proliferation and apoptosis were determined within the tibial epiphyseal growth plate and primary spongiosa (dashed and solid boxes, respectively). Bars, 500 μm. (B) Representative examples of BrdU incorporation into proliferative zone chondrocytes of the tibial epiphyseal growth plate (arrows) from 6-day-old U+/M+, U−/M+, U+/M−, and U−/M− pups. Sections were counterstained with hematoxylin. Bars, 50 μm. (C) Enumeration of proliferation rates of proliferative zone chondrocytes from U+/M+, U−/M+, U+/M−, and U−/M− pups. Data are shown as means ± standard errors of the means. **, $P < 0.01$ (Student's $t$ test, two tailed). N, number of mice included in each measurement. (D) Apoptotic cells (arrows) as detected by terminal deoxynucleotidyltransferase-mediated dUTP-biotin nick end labeling (Tunel) staining of primary spongiosa of the tibias of 6-day-old U+/M+, U−/M+, U+/M−, and U−/M− pups. Bars, 50 μm. Sections were counterstained with contrast green. (E) Enumeration of apoptotic indices of the primary spongiosa from U+/M+, U−/M+, U+/M−, and U−/M− mice. Data are shown as means ± standard errors of the means. *, $P < 0.05$ (Student's $t$ test, two tailed). N, number of mice included in each measurement.

turnover and pericellular collagen turnover promote cell growth and cell survival in a collagen-rich microenvironment in a functionally complementary manner.

## DISCUSSION

Intracellular collagen degradation was recognized as a pathway for the turnover of this abundant extracellular matrix component more than three decades ago (7, 9, 15). However, due to the lack of means to manipulate the cellular uptake of collagen in experimental animals, limited information with respect to both the role of this pathway in physiological and pathological processes and its mechanistic relationship to other collagen turnover pathways is available. The recent generation of mice with a specific defect in the cellular uptake of collagen has provided a unique opportunity to analyze funda-

mental aspects of the biology of the intracellular collagen degradation pathway. Here we studied the physiological functions of uPARAP/Endo180 in intracellular collagen degradation in vivo. We found that the expression of uPARAP/Endo180 was largely restricted to bone and other hard tissues in the early postnatal period and that the uPARAP/Endo180-dependent collagen degradation pathway was operative in both chondrocytes and osteoblasts. This suggested a key physiological function of uPARAP/Endo180-mediated intracellular collagen turnover in the development of these collagen-rich tissues. Indeed, the comprehensive analysis of uPARAP/Endo180-deficient bones performed in this study revealed a number of defects in bone development of uPARAP/Endo180-deficient mice. These were similar to, although less severe than, the bone development defects observed after the ablation of MT1-MMP. Because of the conspicuously similar patterns of expression of uPARAP/Endo180 and MT1-MMP in developing bone, the strict requirement of MT1-MMP for pericellular collagen degradation by chondrocytes and osteoblasts, and the previous demonstration of a dramatic increase in intracellular collagen in bone cells from M− mice (19, 45), this provided an opportunity to determine if functional deficits in intracellular collagen degradation could be compensated by collagen degradation in the pericellular environment and vice versa. Indeed, we found that combined deficiencies in uPARAP/Endo180 and MT1-MMP strongly exacerbated the defects arising from a single deficiency in either uPARAP/Endo180 or MT1-MMP. Importantly, the combined loss of uPARAP/Endo180 and MT1-MMP synergistically impaired the ability of cells to proliferate and survive in the collagen-rich microenvironment of the developing bone. As a consequence, mice with combined uPARAP/Endo180 and MT1-MMP deficiencies formed small and poorly mineralized bones. These skeletal abnormalities likely caused the uniform postnatal death of double-deficient pups, based on the normal appearance of the soft tissues of uPARAP/Endo180 and MT1-MMP double-deficient mice and the general absence of uPARAP/Endo180 expression in soft tissues within the postnatal period. The ultimate cause of death of double-deficient mice secondary to poor bone formation remains undetermined. Likely scenarios include failure of the rib cage to adequately support respiration of rapidly growing pups, head trauma inflicted by nursing mothers when manipulating pups during transportation or cleaning, parental cannibalism, or combinations thereof.

The findings presented here demonstrate that a molecular plasticity exists in the turnover of collagen associated with bone formation and likely in other physiological and pathological tissue-remodeling processes. The data provide direct experimental support for our previous speculation that the two pathways for the turnover of collagen (intracellular and pericellular) can act in a complementary manner during physiological and pathological tissue remodeling (11, 19). By inference, this implies that pharmacological prevention of the pathological destruction of collagen during the progression of degenerative diseases may be most efficiently achieved through the inhibition of both intracellular and pericellular pathways, although this also could increase the risk of undesired side effects. In this respect, it is important to note that intracellular inclusions of phagocytosed collagen have been observed in connective tissue cells associated with cancer, rheumatoid arthritis, emphysema, and periodontal disease, suggesting that the intracellular collagen degradation pathway is active in these human diseases (7, 8, 17, 27, 31, 37). Our data also lend support to a recent proposal that matrix metalloproteinase inhibitors may have been ineffective in blocking tumor extracellular matrix and basement membrane degradation, at least partially due to the unimpeded functionality of an intracellular, non-MMP-dependent pathway (32).

The specific reasons for the strong synergistic effect of combined uPARAP/Endo180 and MT1-MMP deficiency on cell proliferation and survival in developing bones remain to be determined. uPARAP/Endo180 expression is strictly confined to cells of the osteoblast/osteocyte lineage and chondrocytes of developing bone, and the receptor was not expressed by endothelial cells, either in the developing bones or at other anatomical sites (data not shown). The inability of resident cells with combined uPARAP/Endo180 and MT1-MMP deficiencies (chondrocyte/osteoblasts) to remodel collagen may lead to a failure to create a microenvironment that is conducive to their survival and growth, either due to physical constraints imposed by the collagen, failure to liberate latent growth factors and bioactive extracellular matrix fragments, or combinations thereof.

In summary, our studies demonstrate that both intracellular and pericellular collagen turnover pathways participate in physiological tissue remodeling, that both promote the survival and proliferation of cells located in a collagen-rich microenvironment, and that these two pathways can act in a complementary manner.

## ACKNOWLEDGMENTS

We thank Mary Jo Danton for carefully reading the manuscript, Yanming Bi for help with computer tomography, and Ludmila Szobova for chondrocyte preparations.

This work was supported by the NIDCR Intramural Research Program and by a grant from the Department of Defense (DAMD-17-02-0693) to Thomas H. Bugge. Lars H. Engelholm and Niels Behrendt were supported by EU contract LSHC-CT-2003-503297 and by grants from the Danish Cancer Society, the Danish Cancer Research Foundation, and the Danish Medical Research Council.

## REFERENCES

1. **Baker, A. H., D. R. Edwards, and G. Murphy.** 2002. Metalloproteinase inhibitors: biological actions and therapeutic opportunities. J. Cell Sci. **115:** 3719–3727.
2. **Beertsen, W., K. Holmbeck, A. Niehof, P. Bianco, K. Chrysovergis, H. Birkedal-Hansen, and V. Everts.** 2003. Inhibition of molar eruption and root elongation in MT1-MMP-deficient mice. Connect. Tissue Res. **44**(Suppl. 1)**:**298–299.
3. **Behrendt, N., O. N. Jensen, L. H. Engelholm, E. Mortz, M. Mann, and K. Dano.** 2000. A urokinase receptor-associated protein with specific collagen binding properties. J. Biol. Chem. **275:**1993–2002.
4. **Birkedal-Hansen, H.** 1987. Catabolism and turnover of collagens: collagenases. Methods Enzymol. **144:**140–171.
5. **Chun, T. H., K. B. Hotary, F. Sabeh, A. R. Saltiel, E. D. Allen, and S. J. Weiss.** 2006. A pericellular collagenase directs the 3-dimensional development of white adipose tissue. Cell **125:**577–591.
6. **Coussens, L. M., B. Fingleton, and L. M. Matrisian.** 2002. Matrix metalloproteinase inhibitors and cancer: trials and tribulations. Science **295:**2387–2392.
7. **Cullen, J. C.** 1972. Intracellular collagen in experimental arthritis in rats. J. Bone Joint Surg. Br. **54:**351–359.
8. **Curino, A. C., L. H. Engelholm, S. S. Yamada, K. Holmbeck, L. R. Lund, A. A. Molinolo, N. Behrendt, B. S. Nielsen, and T. H. Bugge.** 2005. Intracellular collagen degradation mediated by uPARAP/Endo180 is a major pathway of extracellular matrix turnover during malignancy. J. Cell Biol. **169:** 977–985.
9. **Dyer, R. F., and R. D. Peppler.** 1977. Intracellular collagen in the nonpregnant and IUD-containing rat uterus. Anat. Rec. **187:**241–247.

10. **East, L., A. McCarthy, D. Wienke, J. Sturge, A. Ashworth, and C. M. Isacke.** 2003. A targeted deletion in the endocytic receptor gene Endo180 results in a defect in collagen uptake. EMBO Rep. **4:**710–716.
11. **Engelholm, L. H., K. List, S. Netzel-Arnett, E. Cukierman, D. J. Mitola, H. Aaronson, L. Kjoller, J. K. Larsen, K. M. Yamada, D. K. Strickland, K. Holmbeck, K. Dano, H. Birkedal-Hansen, N. Behrendt, and T. H. Bugge.** 2003. uPARAP/Endo180 is essential for cellular uptake of collagen and promotes fibroblast collagen adhesion. J. Cell Biol. **160:**1009–1015.
12. **Engelholm, L. H., B. S. Nielsen, S. Netzel-Arnett, H. Solberg, X. D. Chen, J. M. Lopez Garcia, C. Lopez-Otin, M. F. Young, H. Birkedal-Hansen, K. Dano, L. R. Lund, N. Behrendt, and T. H. Bugge.** 2001. The urokinase plasminogen activator receptor-associated protein/endo180 is coexpressed with its interaction partners urokinase plasminogen activator receptor and matrix metalloprotease-13 during osteogenesis. Lab. Investig. **81:**1403–1414.
13. **Everts, V., R. M. Hembry, J. J. Reynolds, and W. Beertsen.** 1989. Metalloproteinases are not involved in the phagocytosis of collagen fibrils by fibroblasts. Matrix **9:**266–276.
14. **Everts, V., E. van der Zee, L. Creemers, and W. Beertsen.** 1996. Phagocytosis and intracellular digestion of collagen, its role in turnover and remodelling. Histochem. J. **28:**229–245.
15. **Garant, P. R.** 1976. Collagen resorption by fibroblasts. A theory of fibroblastic maintenance of the periodontal ligament. J. Periodontol. **47:**380–390.
16. **Gelb, B. D., G. P. Shi, H. A. Chapman, and R. J. Desnick.** 1996. Pycnodysostosis, a lysosomal disease caused by cathepsin K deficiency. Science **273:** 1236–1238.
17. **Harris, E. D., Jr., A. M. Glauert, and A. H. Murley.** 1977. Intracellular collagen fibers at the pannus-cartilage junction in rheumatoid arthritis. Arthritis Rheum. **20:**657–665.
18. **Havemose-Poulsen, A., P. Holmstrup, K. Stoltze, and H. Birkedal-Hansen.** 1998. Dissolution of type I collagen fibrils by gingival fibroblasts isolated from patients of various periodontitis categories. J. Periodontal Res. **33:**280–291.
19. **Holmbeck, K., P. Bianco, J. Caterina, S. Yamada, M. Kromer, S. A. Kuznetsov, M. Mankani, P. G. Robey, A. R. Poole, I. Pidoux, J. M. Ward, and H. Birkedal-Hansen.** 1999. MT1-MMP-deficient mice develop dwarfism, osteopenia, arthritis, and connective tissue disease due to inadequate collagen turnover. Cell **99:**81–92.
20. **Holmbeck, K., P. Bianco, K. Chrysovergis, S. Yamada, and H. Birkedal-Hansen.** 2003. MT1-MMP-dependent, apoptotic remodeling of unmineralized cartilage: a critical process in skeletal growth. J. Cell Biol. **163:**661–671.
21. **Holmbeck, K., P. Bianco, I. Pidoux, S. Inoue, R. C. Billinghurst, W. Wu, K. Chrysovergis, S. Yamada, H. Birkedal-Hansen, and A. R. Poole.** 2005. The metalloproteinase MT1-MMP is required for normal development and maintenance of osteocyte processes in bone. J. Cell Sci. **118:**147–156.
22. **Hotary, K. B., E. D. Allen, P. C. Brooks, N. S. Datta, M. W. Long, and S. J. Weiss.** 2003. Membrane type I matrix metalloproteinase usurps tumor growth control imposed by the three-dimensional extracellular matrix. Cell **114:**33–45.
23. **Inada, M., Y. Wang, M. H. Byrne, M. U. Rahman, C. Miyaura, C. Lopez-Otin, and S. M. Krane.** 2004. Critical roles for collagenase-3 (Mmp13) in development of growth plate cartilage and in endochondral ossification. Proc. Natl. Acad. Sci. USA **101:**17192–17197.
24. **Kjoller, L., L. H. Engelholm, M. Hoyer-Hansen, K. Dano, T. H. Bugge, and N. Behrendt.** 2004. uPARAP/endo180 directs lysosomal delivery and degradation of collagen IV. Exp. Cell Res. **293:**106–116.
25. **Lee, H., C. M. Overall, C. A. McCulloch, and J. Sodek.** 2006. A critical role for MT1-MMP in collagen phagocytosis. Mol. Biol. Cell **17:**4812–4826.
26. **Linsenmayer, T. F.** 1991. Collagen. Plenum Press, New York, NY.
27. **Lucattelli, M., E. Cavarra, M. M. de Santi, T. D. Tetley, P. A. Martorana, and G. Lungarella.** 2003. Collagen phagocytosis by lung alveolar macrophages in animal models of emphysema. Eur. Respir. J. **22:**728–734.
28. **Matsuki, Y., M. Nakashima, N. Amizuka, H. Warshawsky, D. Goltzman, K. M. Yamada, and Y. Yamada.** 1995. A compilation of partial sequences of randomly selected cDNA clones from the rat incisor. J Dent. Res. **74:**307–312.
29. **Mohamed, M. M., and B. F. Sloane.** 2006. Cysteine cathepsins: multifunctional enzymes in cancer. Nat. Rev. Cancer **6:**764–775.
30. **Mott, J. D., and Z. Werb.** 2004. Regulation of matrix biology by matrix metalloproteinases. Curr. Opin. Cell Biol. **16:**558–564.
31. **Neurath, M. F.** 1993. Detection of Luse bodies, spiralled collagen, dysplastic collagen, and intracellular collagen in rheumatoid connective tissues: an electron microscopic study. Ann. Rheum. Dis. **52:**278–284.
32. **Overall, C. M., and O. Kleifeld.** 2006. Tumour microenvironment—opinion: validating matrix metalloproteinases as drug targets and anti-targets for cancer therapy. Nat. Rev. Cancer **6:**227–239.
33. **Saftig, P., E. Hunziker, O. Wehmeyer, S. Jones, A. Boyde, W. Rommerskirch, J. D. Moritz, P. Schu, and K. von Figura.** 1998. Impaired osteoclastic bone resorption leads to osteopetrosis in cathepsin-K-deficient mice. Proc. Natl. Acad. Sci. USA **95:**13453–13458.
34. **Sato, H., T. Takino, Y. Okada, J. Cao, A. Shinagawa, E. Yamamoto, and M. Seiki.** 1994. A matrix metalloproteinase expressed on the surface of invasive tumour cells. Nature **370:**61–65.
35. **Schnack Nielsen, B., F. Rank, L. H. Engelholm, A. Holm, K. Dano, and N. Behrendt.** 2002. Urokinase receptor-associated protein (uPARAP) is expressed in connection with malignant as well as benign lesions of the human breast and occurs in specific populations of stromal cells. Int. J. Cancer **98:**656–664.
36. **Sheikh, H., H. Yarwood, A. Ashworth, and C. M. Isacke.** 2000. Endo180, an endocytic recycling glycoprotein related to the macrophage mannose receptor is expressed on fibroblasts, endothelial cells and macrophages and functions as a lectin receptor. J. Cell Sci. **113:**1021–1032.
37. **Soames, J. V., and R. M. Davies.** 1977. Intracellular collagen fibrils in early gingivitis in the beagle dog. J. Periodontal Res. **12:**378–386.
38. **Stickens, D., D. J. Behonick, N. Ortega, B. Heyer, B. Hartenstein, Y. Yu, A. J. Fosang, M. Schorpp-Kistner, P. Angel, and Z. Werb.** 2004. Altered endochondral bone development in matrix metalloproteinase 13-deficient mice. Development **131:**5883–5895.
39. **van der Rest, M., and R. Garrone.** 1991. Collagen family of proteins. FASEB J. **5:**2814–2823.
40. **Watanabe, H., and Y. Yamada.** 1999. Mice lacking link protein develop dwarfism and craniofacial abnormalities. Nat. Genet. **21:**225–229.
41. **Wienke, D., J. R. MacFadyen, and C. M. Isacke.** 2003. Identification and characterization of the endocytic transmembrane glycoprotein Endo180 as a novel collagen receptor. Mol. Biol. Cell **14:**3592–3604.
42. **Windsor, L. J., A. Havemose-Poulsen, S. Yamada, J. G. Lyons, B. Birkedal-Hansen, W. G. Stetler-Stevenson, and H. Birkedal-Hansen.** 2002. Matrix metalloproteinases, p. 10.8. *In* K. Morgan (ed.), Current protocols in cell biology, vol. 10. Wiley & Sons, Inc., New York, NY.
43. **Wu, K., J. Yuan, and L. A. Lasky.** 1996. Characterization of a novel member of the macrophage mannose receptor type C lectin family. J. Biol. Chem. **271:**21323–21330.
44. **Yamada, K. M.** 2003. Cell biology: tumour jailbreak. Nature **424:**889–890.
45. **Zhou, Z., S. S. Apte, R. Soininen, R. Cao, G. Y. Baaklini, R. W. Rauser, J. Wang, Y. Cao, and K. Tryggvason.** 2000. Impaired endochondral ossification and angiogenesis in mice deficient in membrane-type matrix metalloproteinase I. Proc. Natl. Acad. Sci. USA **97:**4052–4057.